CHAPTER 5

EFFECT OF AN ENCOUNTER ON A GFD

5.1 Review of the impulse approximation

When two galaxies encounter each other at high relative speeds the effect of the encounter on the gross features of each galaxy such as energy and angular momentum can be estimated analytically. The nature of the approximation is as follows. If the relative speed between the galaxies is large enough, the effective duration of the encounter is short when compared to typical orbital (or dynamical) times for stars within each galaxy. Then, it is reasonable to suppose that during the encounter stars (relative to the centres of their galaxy) have not moved appreciably. Having frozen the stars, it is straightforward to calculate the "impulse" (change in velocity) given to each star as a result of the encounter. During the encounter, the centres of the galaxies are assumed to move in Keplerian hyperbolae. We shall also show that within the impulse approximation theory, straight line trajectories are a good approximation.

Let the galaxies have masses M_1 and M_2 and median radii r_1 and r_2. Then, the orbital timescales within the galaxies are.

$$t_1 \sim \frac{r_1^{3/2}}{(GM_1)^{1/2}} \quad , \quad t_2 \sim \frac{r_2^{3/2}}{(GM_2)^{1/2}} \qquad (5.1)$$

Suppose now that the galaxies undergo an encounter and at the instant of closest approach let b be the separation between their centres and V, the relative speed. The effective duration of the encounter is

$$t_{enc} \sim \frac{max(r_1, r_2, b)}{V} \qquad (5.2)$$

We treat the encounter as impulsive when

$$t_{enc} \ll min(t_1, t_2) \qquad (5.3)$$

While using the impulse approximation, we assume that the density distribution in each galaxy remains unaltered during the encounter. Hence we may treat the galaxies as rigid bodies with their centres moving in Keplerian hyperbolae. A simple argument shows that the hyperbolic trajectory of the reduced mass can be approximated by a straight line trajectory. If θ is the deflection angle of the reduced mass then

$$\tan(\theta/2) = \frac{G(M_1 + M_2)}{p V_\infty^2} \qquad (5.4)$$

where p is the impact parameter and V_∞ is the relative speed at infinity. Since $b < p$ and $V_\infty^2 = V^2 - \frac{2G(M_1+M_2)}{b}$, we have

$$\tan(\theta/2) \quad \frac{1}{\frac{bV^2}{G(M_1+M_2)} - 2} \qquad (5.5)$$

From (5.1) $G(M_1+M_2) \sim r_1^3/t_1^2 + r_2^3/t_2^2$

Let us suppose that $b > \max(r_1, r_2)$. Then with $t_{enc} \sim b/V$ we have

$$\frac{bV^2}{G(M_1+M_2)} \sim \frac{bV^2}{\frac{r_1^3}{t_1^2}+\frac{r_2^3}{t_2^2}} \sim \frac{b^3/t_{enc}^2}{\frac{r_1^3}{t_1^2}+\frac{r_2^3}{t_2^2}}$$

From (5.3), since $t_{enc} \ll \min(t_1, t_2)$

$$\frac{bV^2}{G(M_1+M_2)} \gg 1$$

Therefore $\tan(\theta/2) \sim 0$ implying that the relative separation vector is hardly deflected from a straight line path. Also the impact parameter (p) is very nearly equal to b.

Let the centres of M_1 and M_2 move in the (x-y) plane and let the position vector of the centre of M_2 (the perturbing galaxy) with respect to the centre of M_1 (the perturbed galaxy) be given by

$$\underline{R} \simeq (b, Vt, 0) \qquad (5.6)$$

Let $\underline{\Delta V_j'}$ be the change in velocity of the jth star belonging to the galaxy with mass M_1 due to the impulse given to it by M_2. The total momentum transferred to M_1 is $\sum_j m_j \underline{\Delta V_j'}$

where m_j is the mass of the jth star ($\sum_j m_j = M_1$). Therefore the change in the velocity of the centre of mass of M_1 is

$$\underline{\Delta V_{cm}} = \frac{1}{M_1} \sum_j m_j \underline{\Delta V_j'} \qquad (5.7)$$

The change in velocity of the jth star with respect to the centre of mass of M_1 is

$$\underline{\Delta V_j} = \underline{\Delta V_j'} - \underline{\Delta V_{cm}} \qquad (5.8)$$

We can write down an explicit expression for $\underline{\Delta V_j}$ in terms of the approximate orbit (5.6) of M_2. If $\underline{F}(\underline{r}, t)$ is the force per unit mass (at position $\underline{r}$ with respect to the centre of M_1) due to M_2 at time t, then

$$\underline{\Delta V_j'} = \int_{-\infty}^{\infty} \underline{F}(\underline{r_j}, t)\, dt \qquad (5.9a)$$

and

$$\underline{\Delta V_j} = \int_{-\infty}^{\infty} \left\{ \underline{F}(\underline{r_j}, t) - \frac{1}{M_1} \sum_k m_k \underline{F}(\underline{r_k}, t) \right\} dt \qquad (5.9b)$$

Having calculated $\underline{\Delta V_j}$, we estimate the change in the internal energy and angular momentum of M_1. Since the potential energy of M_1 does not change during the encounter, the change in the internal energy equals the internal kinetic energy imparted to M_1 which is

$$\Delta E = \frac{1}{2} \sum_k m_k \left\{ (\underline{V_k} + \underline{\Delta V_k})^2 - V_k^2 \right\}$$

where V_k is the velocity of the kth star before the encounter.

$$\Delta E = \sum_k m_k \left(\underline{V_k} \cdot \underline{\Delta V_k} \right) + \frac{1}{2} \sum_k m_k \left(\underline{\Delta V_k} \right)^2 \qquad (5.10)$$

We note that the first term (which is linear in $\underline{\Delta V_k}$) vanishes when there is no streaming motion within the unperturbed galaxy. Also, it can be shown that since $\underline{F}$ is derivable from a potential i.e. $F = -\nabla\varphi$), $\sum m_k \left(\underline{V_k} \cdot \underline{\Delta V_k} \right)$ vanishes, by symmetry, for an axisymmetric galaxy. Therefore the galaxy gains internal energy

$$\Delta E = \frac{1}{2} \sum_k m_k \left| \underline{\Delta V_k} \right|^2 \qquad (5.11)$$

Also the change in angular momentum is

$$\underline{\Delta L} = \sum_k m_k \left(\underline{r_k} \times \underline{\Delta V_k} \right) \qquad (5.12)$$

When the galaxy gains ΔE (5.11) as pure internal kinetic energy, it is disturbed from its equilibrium state. The process of readjustment to a new equilibrium involves considering how much mass and energy are lost from the system (see eg. Aguilar & White, 1985 and references therein for a discussion of these issues).

5.2 The tidal approximation

Let $\underline{R}$ be the position vector (at some instant of time t) of the centre of M_2 with respect to the centre of M_1. We can expand the force per unit mass at position (from the centre of M_1) due to M_2 in a Taylor series.

$$\underline{F}(\underline{r};\underline{R}) = \underline{F}(0;\underline{R}) + (\underline{r}\cdot\nabla)\underline{F}\Big|_{\underline{r}=0} + O\left(\frac{r^2}{R^2}\right) \quad (5.13)$$

The first term gives the acceleration of the centre of mass of M_1 while the second term (to first order in $\frac{r}{R}$) is the tidal force acting on M_1. In the (first order) tidal approximation only these terms are retained. It is clear that the tidal approximation is quite independent of the impulse approximation. But when they are combined one obtains a simple and useful expression for the impulse ($\Delta\underline{V}(\underline{r})$).

5.3 The impulse + tidal approximation

Let us suppose that M_2 is a point mass whose position vector ($\underline{R}$) with respect to the centre of M_1 moves according to *(5.6)*:

$$\underline{R}(t) = (b, Vt, 0)$$

Then

$$\underline{F}(\underline{r};\underline{R}) = \frac{GM_2(\underline{R}-\underline{r})}{|\underline{R}-\underline{r}|^3} \quad (5.14)$$

In the first order tidal approximation (5.13)

$$\underline{F}(\underline{r};\underline{R}) \simeq \frac{GM_2}{R^3}\underline{R} + \left\{\frac{3\underline{R}(\underline{R}\cdot\underline{r})}{R^5} - \frac{\underline{r}}{R^3}\right\} \qquad (5.15)$$

Using (5.15) and (5.6) in (5.9) we get

$$\underline{\Delta V}(\underline{r}) \simeq \frac{2GM_2}{b^2V}(x, 0, -z) \qquad (5.16)$$

If $\rho(\underline{r})$ is the density distribution of (the unperturbed) M_1, using the expression for $\underline{\Delta V}(\underline{r})$ from (5.16) in the expressions (5.11 and 5.12) for ΔE and $\underline{\Delta L}$, we get

$$\Delta E = \frac{2G^2M_2^2}{b^4V^2}\int (x^2+z^2)\rho(\underline{r})\, d^3r \qquad (5.17a)$$

$$\underline{\Delta L} = \frac{2GM_2}{b^2V}\int \left\{\hat{x}(-yz) + \hat{y}(2xz) + \hat{z}(-xy)\right\}\rho(\underline{r})\, d^3r \qquad (5.17b)$$

For a spherically symmetric system

$$\int (x^2+z^2)\rho(\underline{r})\, d^3r = \frac{2}{3}\int r^2\rho(\underline{r})\, d^3r$$

Defining the mean square radius of M_1 as

$$\overline{r^2} = \frac{1}{M_1}\int r^2\rho(\underline{r})\, d^3r \qquad (5.18)$$

we write

$$\Delta E = \frac{2G^2 M_2^2 M_1}{b^4 V^2} \overline{r^2} \qquad (5.19)$$

Therefore the most effective encounters are those which are slow and close - precisely the cases for which the impulse plus tidal approximation can be expected to fail. Even if the encounter is fast and distant, ΔE can be large if M_2 is large. We note that the only properties of the perturbed galaxy that enter (5.197 are its total mass and mean square radius. In particular the impulse + tidal approximation predicts that the velocity space distribution of the perturbed galaxy does not determine the energy transfer in most cases of interest - the exceptions being those for which the linear term in ΔV in (5.10) makes a nonzero contribution. For most galaxy models $\overline{xy}$, $\overline{yz}$, $\overline{zx}$ are zero. Therefore ΔL in (5.17b) is expected to be zero.

5.4 The tidally forced GFD

It is quite easy to relax the assumptions of a point mass perturber and of a distant encounter (ie. the first order tidal approximation). Results for these more general cases are reviewed by Alladin and Narasimhan (1982). However, it is much more difficult to go beyond the impulse approximation. An exception is the work by Palmer and Papaloizou (1982). They studied the effect of a slow encounter on a rotating disc in an approximation that went beyond the impulse approximation, but one which neglected the

changes in the self gravity of the disc during the encounter.

We present an analytic model of the effect of an encounter on a galaxy which has the following features.

(i) The perturbed galaxy is a GFD.

(ii) The perturber moves in the plane of the GFD.

(iii) The tidal forces on the GFD are truncated at first order as in (5.13).

The return for confining oneself to these special circumstances is that one obtains a set of ordinary differential equations for the (10) parameters of the GFD. The numerical work involved in integrating this model is trivial compared to that needed in a full N-body code. This model goes beyond the study by Palmer and Papaloizou (1982) in that the fully self consistent response of the GFD is retained, although it is restricted to harmonic forces.

Below we summarize the construction of GFDs which was discussed in detail in chapter 4. Then we show how to include the effect of the tidal field of a perturber (on the GFD) moving in the plane of the GFD.

5.4a Summary of the construction of **GFDs**

(i) GFDs are described by phase space distribution functions which have the form

$$f_{GFD} = f_0 \left(1 - I\right)^{-1/2}$$

where $I = Z^T Q Z$ is a positive definite quadratic form in $Z = (x, y, V_x, V_y)^T$ [Q is a positive definite 4 x

real symmetric matrix].

(ii) Integrating f_{GFD} over V_x and V_y, the surface density

$$\sum \propto (1 - q(t))^{1/2}$$

where $q(t)$ is a positive definite quadratic form in x and y.

(iii) The interior gravitational force due to $\sum$ is linear in x and y. The resulting linearity of the equations of motion ($\dot{Z} = KZ$) for a star belonging to the **GDF** allowed us to construct the integral of motion .

(iv) I = an integral of motion implies that Q obeys

$$\dot{Q} = -K^T Q - QK$$

(v) This equation for Q is more conveniently written in terms of $P = Q^{-1}$ since the elements of P are averages of phase space coordinates like x^2, xy, xV_x etc.

$$\dot{P} = KP + PK^T$$

(vi) K is determined self consistently from P itself:

$$K = \begin{bmatrix} O_{2\times 2} & \mathbb{I}_{2\times 2} \\ -\mathbb{F} & O_{2\times 2} \end{bmatrix}$$

where $\mathbb{F}$ is the 2 x 2 matrix containing the "**strengths**" of the force of self gravity as given in **(4.27)** and **(4.35).**

5.4b Including the tidal field **of a** perturber

We recall **(4.24)** that the internal gravitational potential of a GFD can be written as

$$\varphi(x,y,t) = \frac{\alpha}{2}x^2 + \beta xy + \frac{\gamma}{2}y^2$$

where α, β and γ are time dependent.

From **(4.27)** and **(4.35)**

$$\mathbb{F} = \begin{pmatrix} \alpha & \beta \\ \beta & \gamma \end{pmatrix}$$

$$\alpha = A^2\cos^2\theta + B^2\sin^2\theta$$

$$\beta = (A^2 - B^2)\sin\theta\cos\theta$$

$$\gamma = A^2\sin^2\theta + B^2\cos^2\theta$$

A (perturbing) galaxy moving in the plane of the GFD exerts tidal forces on **it.** When the variation of this tidal force over the size of the GFD can be well approximated by the first order tidal approximation **(5.13)** we note that the addition of these tidal forces to the self gravity of the GFD preserves the linearity of the equations of motion ($\dot{\mathbb{Z}} = K\mathbb{Z}$). All we need to do is to add the "strengths" of the time dependent tidal force to α, β and γ. The perturber could be the extended halo of another galaxy which is assumed to have a rigid density distribution or **it** could be another GFD whose structure itself could be time varying and coupled to the original GFD. Or again, for simplicity,

the perturber could be a point mass moving in the plane of the GFD. In any case, the motion of the perturber is determined by

$$\ddot{\underline{R}} = \begin{pmatrix}\text{acceleration of the}\\ \text{centre of mass of the}\\ \text{perturber by the GFD}\end{pmatrix} - \begin{pmatrix}\text{acceleration of the}\\ \text{centre of mass of the}\\ \text{GFD by the perturber}\end{pmatrix} \qquad (5.20)$$

where $\underline{R}$ is the separation between the centres of the perturber and the GFD. We note that (5.20) contains the back reaction of the GFD on the orbital motion and allows for energy and angular momentum transfer from the orbital motions of the GFD and the perturber to the internal motions of stars within the GFD.

In particular for a point mass perturber the addition of its tidal field changes

$$\mathbb{F} = \begin{pmatrix}\alpha & \beta\\ \beta & \gamma\end{pmatrix} \quad \text{to} \quad \mathbb{F}' = \begin{pmatrix}\alpha' & \beta'\\ \beta' & \gamma'\end{pmatrix}$$

where

$$\alpha' = \alpha - GM_2\left\{\frac{3(\underline{R}\cdot\hat{x})^2}{R^5} - \frac{1}{R^3}\right\}$$

$$\beta' = \beta - 3GM_2\left\{\frac{(\underline{R}\cdot\hat{x})(\underline{R}\cdot\hat{y})}{R^5}\right\} \qquad (5.21)$$

$$\gamma' = \gamma - GM_2\left\{\frac{3(\underline{R}\cdot\hat{y})^2}{R^5} - \frac{1}{R^3}\right\}$$

The force exerted by the GFD on the point mass depends on the instantaneous shape, size and orientation of the GFD. To

first order in $\left(\frac{\text{GFD SIZE}}{R}\right)$ this force depends only on the position of the centre of mass of the GFD. So we write

$$\ddot{\underline{R}} = -\frac{G(M_1+M_2)}{R^3}\underline{R} \qquad (5.22)$$

which is correct to first order in $\left(\frac{\text{GFD SIZE}}{R}\right)$

5.5 Preliminary numerical studies

We study the response of a GFD to a point mass moving in its plane by numerically integrating (4.22):

$$\dot{P} = K'P + PK'^{T}$$

K' now is given by

$$K' = \begin{pmatrix} O_{2\times 2} & \mathbb{I}_{2\times 2} \\ -\mathbb{F}' & O_{2\times 2} \end{pmatrix} \qquad (5.23)$$

where , which includes both the self gravity of the GFD and the tidal force of the point mass is given in (5.21). The motion of the point mass is governed by (5.22).

Although we could have the pertuber moving along elliptic or circular trajectories around the GFD, in this preliminary study we shall only consider cases when describes hyperbolae. At time = 0 we keep the point mass far away ($R(0) > 50$ x GFD size) from the GFD and choose the GFD itself to be a Kalnajs' disc. Let us recall the form of the phase space distribution function of the Kalnajs disc from section (4.1):

$$f_K(E, L_z) = \left\{ \frac{3M}{4\pi^2 a^4 (\Omega_0^2 - \Omega^2)} \right\} \left[1 + \frac{2(\Omega L_z - E)}{a^2(\Omega_0^2 - \Omega^2)} \right]^{-1/2}$$

$$= \left\{ \frac{3M}{4\pi^2 a^4 (\Omega_0^2 - \Omega^2)} \right\} \left[1 + \frac{2\Omega r V_\theta - V_\theta^2 - V_r^2 - \Omega_0^2 r^2}{a^2(\Omega_0^2 - \Omega^2)} \right]^{-1/2} \quad (5.24)$$

Using

$$\begin{pmatrix} V_r \\ V_\theta \end{pmatrix} = \begin{pmatrix} \cos\theta & \sin\theta \\ -\sin\theta & \cos\theta \end{pmatrix} \begin{pmatrix} V_x \\ V_y \end{pmatrix} \quad (5.25)$$

in (5.24) we can immediately write down the matrix Q_K **as**

$$Q_K = \frac{1}{a^2(\Omega_0^2 - \Omega^2)} \begin{pmatrix} \Omega_0^2 \mathbb{I} & \Omega \mathcal{J} \\ -\Omega \mathcal{J} & \mathbb{I} \end{pmatrix} \quad (5.26)$$

where $\mathbb{I} = \begin{pmatrix} 1 & 0 \\ 0 & 1 \end{pmatrix}$ and $\mathcal{J} = \begin{pmatrix} 0 & -1 \\ 1 & 0 \end{pmatrix}$ (5.27)

We can easily invert Q_K **to get** $P_K = Q_K^{-1}$ **:**

$$P_K = \begin{pmatrix} a^2 \mathbb{I} & -\Omega a^2 \mathcal{J} \\ \Omega a^2 \mathcal{J} & \Omega_0^2 a^2 \mathbb{I} \end{pmatrix} \quad (5.28)$$

Let the point mass perturber pass by with a distance of closest approach = b ($b \gg a$) where its speed is V. Before we describe our results in the next section let us see what the impulse + tidal approximation predicts for the changes in energy and angular momentum of the disc. From (5.16), the impulse transferred is

$$\underline{\Delta V}(x,y) = \frac{2GM_2}{b^2 V}(x,0) \tag{5.29}$$

(the Z component is ignored because the disc always remains confined to the x-y plane).

From (5.17a), the energy gain of the disc is

$$(\Delta E)_{imp} = \frac{2G^2 M_2^2 M_1}{b^4 V^2}\,\overline{x^2}$$

We know from (4.28) and (5.28) that $\overline{x^2} = a^2/5$

Therefore

$$(\Delta E)_{imp} = \frac{2}{5}\,\frac{G^2 M_2^2 M_1}{b^4 V^2}\,a^2 \tag{5.30}$$

From (5.28) we see that $\overline{xy}$ is zero for the Kalnajs disc. Using this fact in the expression for angular momentum transfer, (5.17b), we have

$$(\underline{\Delta L})_{imp} = 0 \tag{5.31}$$

The total energy of the undisturbed Kalnajs' disc is

$$E = -\frac{GM}{5}\,\Omega_0^2 a^2 \qquad (5.32)$$

Defining

(i) dynamical time for the unperturbed disc $= t_{dyn} = \frac{1}{\Omega_0}$

(ii) encounter time $= t_{enc} = b/V$

We can write the fractional energy transfer as

$$\frac{(\Delta E)_{imp}}{|E|} = \frac{32}{9\pi^2}\left(\frac{M_2}{M_{disc}}\right)^2\left(\frac{t_{enc}}{t_{dyn}}\right)^2\left(\frac{a}{b}\right)^6 \qquad (5.33)$$

These are the results in the impulse approximation, which can be compared to the exact calculation for this model described below.

At $t = 0$ the system was chosen to be a Kalnajs' disc of unit mass and radius. The gravitational constant, G, was set equal to unity in all cases. Then $\Omega_0^2 = \frac{3\pi}{4}$ and the only free disc parameter is Ω, the angular rotation velocity. The kinetic and potential energies of the disc do not depend on Ω:

$$\text{Kinetic energy} = T = \frac{3\pi}{20} \qquad (5.34)$$

$$\text{Potential energy} = W = -2T = \frac{3\pi}{10}$$

while the angular momentum (L) is proportional to Ω:

$$L = \frac{2\Omega}{5} \qquad (5.35)$$

The perturber was chosen to be a point mass with mass $M_2 = 2000$. It was set on a (Keplerian) hyperbolic trajectory with a distance of closest approach, $b = 20$. Since the perturber is on a hyperbolic trajectory, there is a certain maximum angle, φ_{max}, which its asymptotic velocity at $t = \infty$ makes with the line joining the centre of the disc and the point of closest approach:

$$\varphi_{max} = \cos^{-1}\left(-\frac{1}{\text{eccentricity}}\right) \; ; \quad \varphi_{max} > \pi/2 \text{ for an unbounded orbit.} \tag{5.36}$$

At $t = 0$, the perturber was chosen to be at $(-0.9\,\varphi_{max})$. The speed at closest approach was varied from its minimum allowed value $\left(V_{min} = \left(\frac{2G(M_1+M_2)}{b}\right)^{1/2} \simeq 14.14567\right)$ - for parabolic orbits - to quite large values. The response of the disc was monitored by solving (5.23) numerically for a period of time in which the perturber moved from $\varphi = -0.9\,\varphi_{max}$ to $\varphi = 0.9\,\varphi_{max}$. The program that solves (5.23) numerically is described in Appendix D where, now, the tidal field of the perturber is also included.

We have performed experiments for the cases $\Omega = +1, 0$ and -1. While the behaviour of the disc itself is an interesting problem that remains to be understood, here, we discuss only the energy and angular momentum changes. Using (5.33) and (5.31) we note that the (impulse plus tidal) approximation predicts

$$\frac{(\Delta E)_{imp}}{|E|} = (0.0225158)\left(\frac{1}{\tau^2}\right) \tag{5.37a}$$

$$(\Delta L)_{imp} = 0 \qquad (5.37b)$$

where $\tau = \frac{t_{dyn}}{t_{enc}} = \frac{V}{b\Omega_0}$ (5.38)

is a dimensionless measure of V.

5.5a Energy transfer

Figures 5.1,5.2 and 5.3 show the fractional energy transfer as a functionof τ for Ω = 10,-1 respectively. The ordinate is

$$Y = \left(\frac{\Delta E}{|E|}\right)\tau^2 \times 100 \qquad (5.39)$$

Then Y_{imp} = 2.25158 for all three figures. We discuss our results briefly below. τ takes values starting from its minimum allowed value of $\tau_{min} = \frac{V_{min}}{b\Omega_0}$ = 0.4608 to values as large as = 25.

The case Ω = 1 (fig.5.1) corresponds to a disc rotating in the same sense as th'e angular velocity of the perturber's orbit. For low encounter speeds, corresponding to small values of τ, the response of the disc is very sensitive to τ. In the range $0.4608 \lesssim \tau \lesssim 0.75$, the energy transfer is almost unpredictable, oscillating wildly from sub-impulsive ($Y < Y_{imp}$) to more than 20 Y_{imp}. We have displayed a few data points in this region. The line joining them is only schematic because the real oscillations of Y are much too wild for sensible display. As τ increases beyond 0.75, the encounter time decreases and the energy

transfer approaches the impulse approximation prediction asymptotically, while always remaining (as far as we can tell) greater than γ_{imp}.

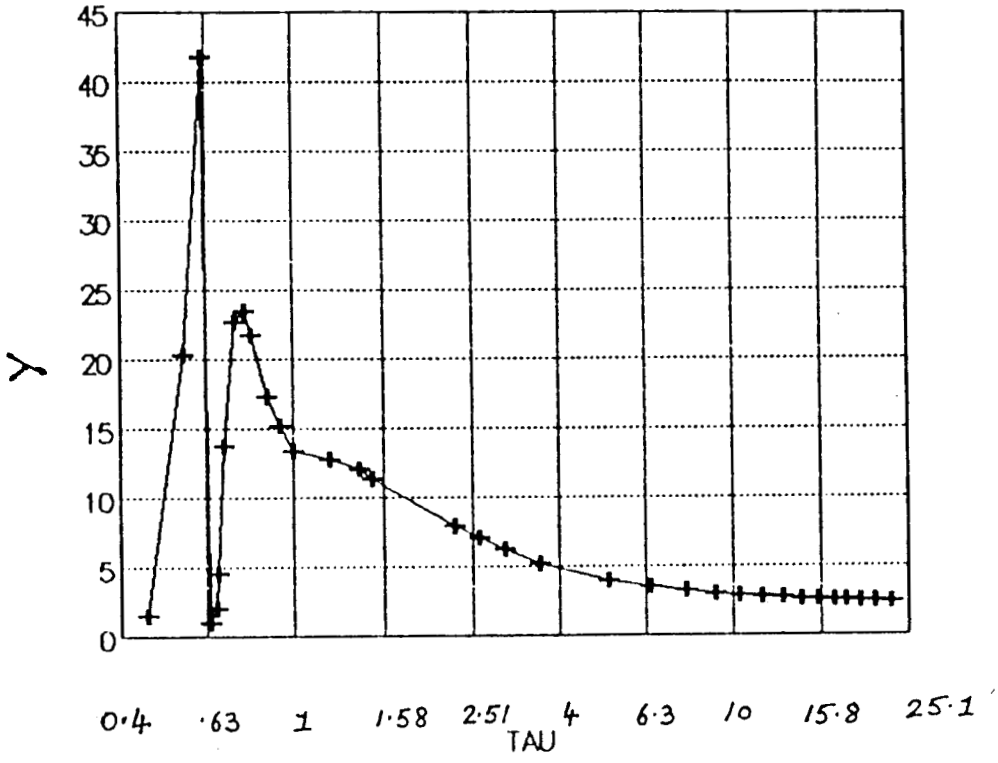

FIGURE 5.1. Energy transfer for $\Omega = 1$

The case $\Omega = -1$ (fig.5.2) corresponds to a counter-rotating disc. This also shows rapid oscillations for $0.4608 \lesssim \tau \lesssim 0.75$ and γ asymptotically approaches γ_{imp}

while always remaining below Y_{imp}.

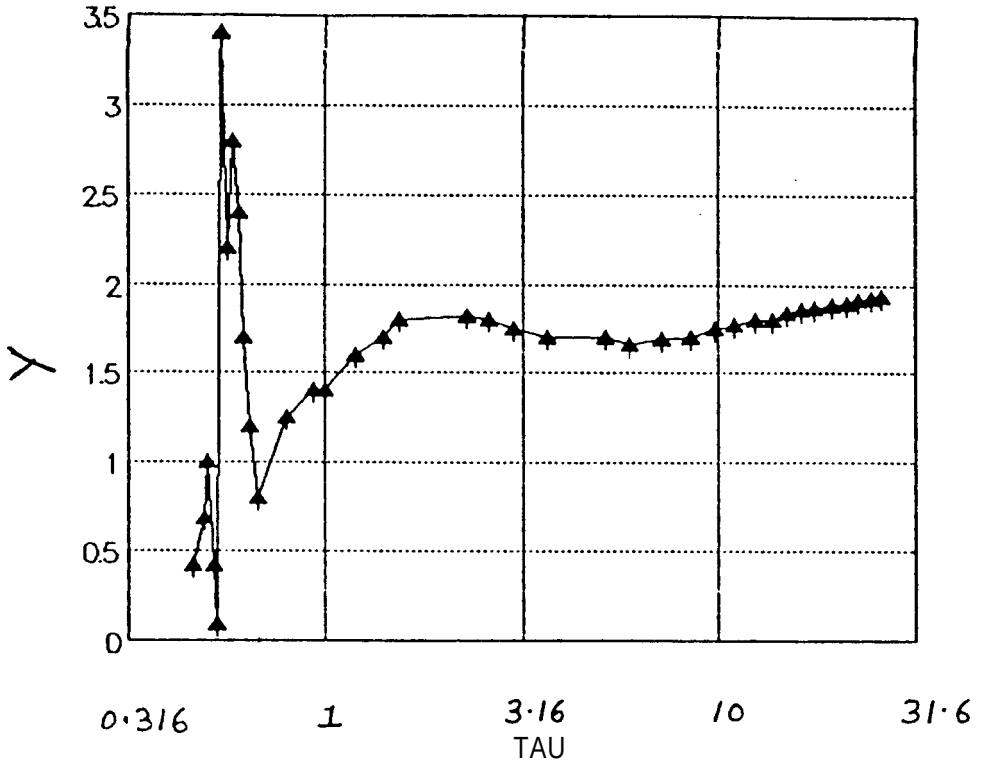

FIGURE 5.2. Energy transfer for $\Omega = -1$

The oscillations of Y for slow encounters is surely due to a resonance between the orbital motion of stars in the disc and the perturber's tidal field. The rapid oscillations are perhaps due to the harmonic (though time dependent) nature of the forces on stars in the GFD. The inclusion of nonlinear terms (in x and y) in the force acting on stars belonging to

more general discs might smooth out these oscillations.

When $\Omega = 0$, the unperturbed Kalnajs' disc is maximally hot. As fig.5.3 shows, the rapid oscillations for small values of τ seen in the cases $\Omega = \pm 1$ are absent here. Instead, γ shows a gentle non monotonic behaviour for these small values of τ. For $\tau \lesssim 1{\cdot}58$, $\left(\frac{\gamma}{\gamma_{imp}}\right) > 2{\cdot}2$ which is a large ($> 100\%$) deviation from that predicted by the impulse approximation. γ generally is greater than γ_{imp} and approaches γ_{imp} rather slowly asymptotically.

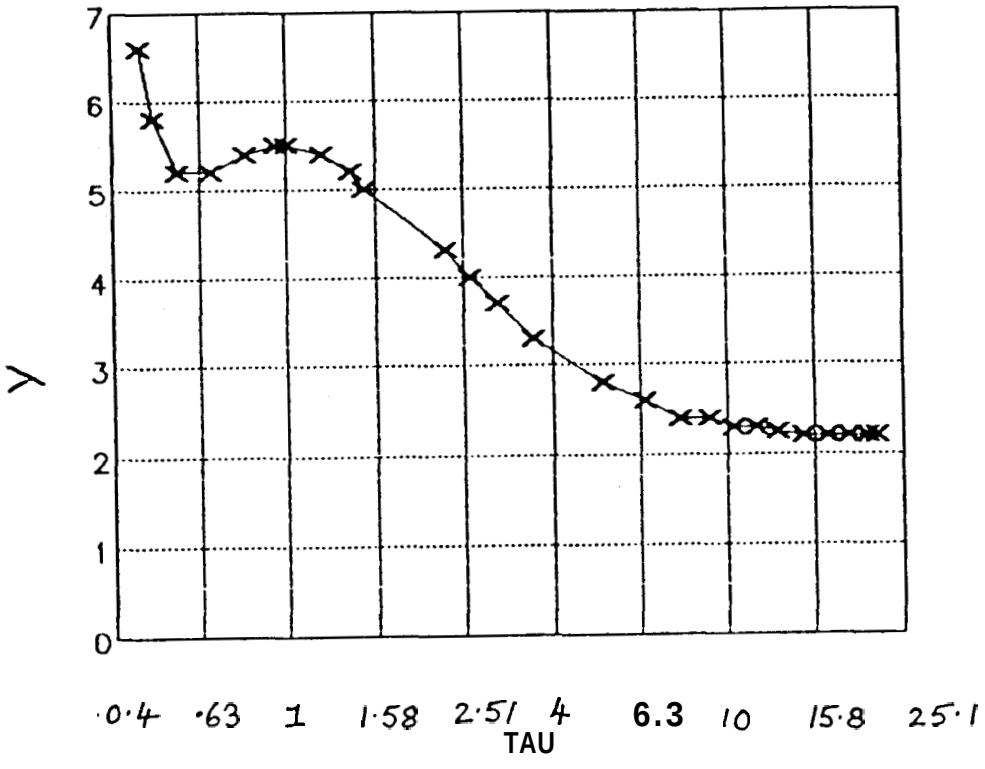

FIGURE 5.3. Energy transfer for $\Omega = 0$

5.5b Angular momentum transfer

For all cases, the angular momentum transfered to the disc increases monotonically as τ decreases from about 24 to 0.8. In this range at any fixed value of τ, ΔL (the angular momentum gain of the GFD) is greatest for the corotating case ($\Omega = 1$) and least for the counterrotating case ($\Omega = -$ 1The details are briefly described below.

Case = 1: The unperturbed disc has $L \square 0.4$. ΔL increases from 2×10^{-6} for τ = 24 to 9.7×10^{-2} for $\tau = 0.8$. As τ is decreased further, A behaves nonmonotonically. This is shown in fig.5.4 below. As before the line is only schematic.

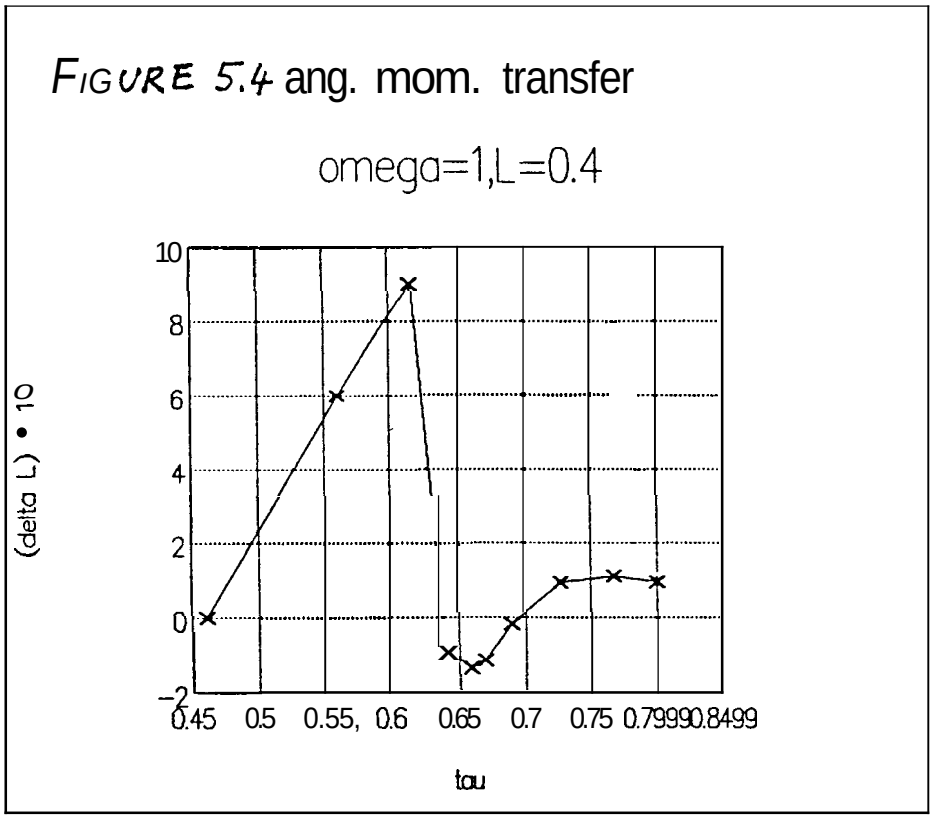

Case $\Omega = 0$: The unperturbed disc has no angular momentum. ΔL seems to increase monotonically from 2.5×10^{-6} for $\tau = 24$ to 0.1 for $\tau = \tau_{min} = 0.4608$.

Case $\Omega = -1$: The unperturbed disc has $L = -0.4$. ΔL increases from 1.4×10^{-6} for $\tau = 24$ to 6×10^{-3} for $\tau = 0.8$. It is nonmonotonic for smaller τ as shown in fig.5.5 below.

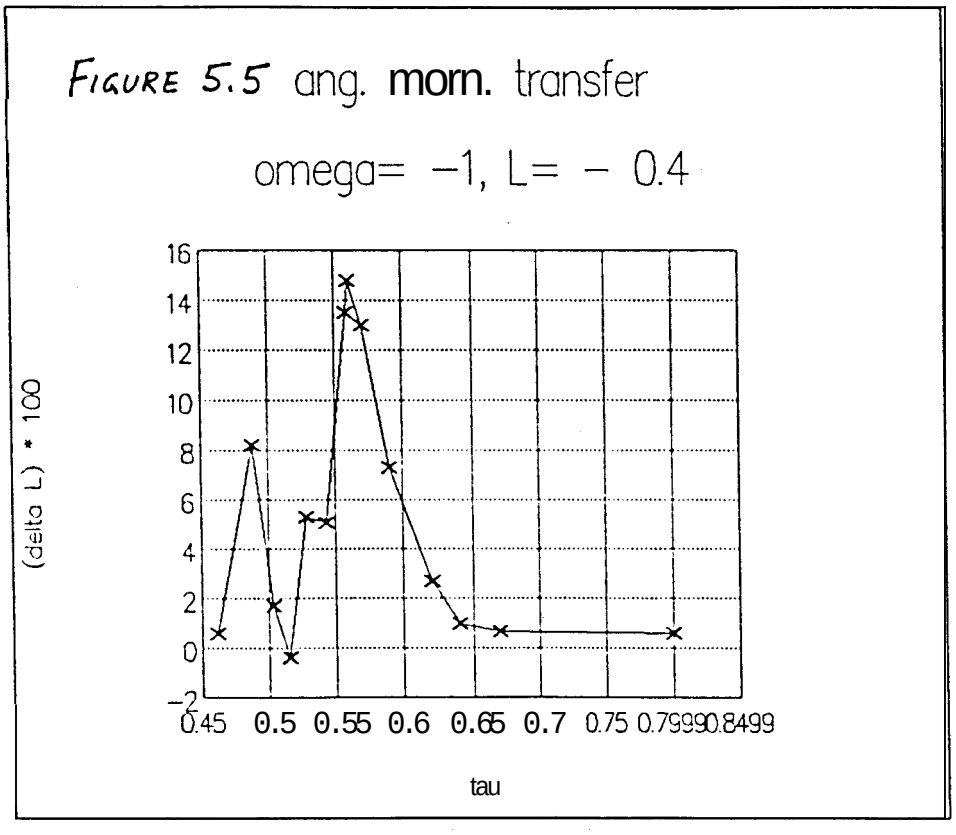

5.6 Discussion

In a different context Subramanian **(1989)** considered the response of a maximally rotating Kalnajs disc to the tidal field of a perturber (in the first order tidal approximation) moving in its plane. The disc itself was assumed to be embedded in a rigid, homogeneous spherical halo. Such a halo introduces an additional potential $\varphi_h = \Omega_h^2 I_2^2$ which can be incorporated in the formalism we have used to describe GFDs. The Kalnajs disc problem studied by Subramanian turns out to be a particular cold case of the interactions of GFDs discussed in this chapter.

The formalism we have set up allows a wide range of intersting situations to be explored. Energy and angular momentum transfer, heating and disruption of a model galaxy by an encounter can be studied. It should be mentioned that there is no post-encounter relaxation in this model. A more realistic model would presumably relax . However, encounters represent behaviour on at most a few dynamical timescales and we are optimistic that this will prove to be a useful guide to the behaviour of more realistic systems.

CHAPTER 6

CONCLUSIONS AND OUTLOOK

This thesis began with the general theme of studying the time dependent behaviour of collisionless self gravitating systems. It is rather hard to obtain exact, general results by analytical methods (see Mathur 1986 for an attempt in the linearised case). The traditional route chosen has been numerical and considerable progress has recently been made in this direction (see eg. Barnes 1989). This approach will certainly allow the study of cases without special symmetry or other simplifying assumptions, at least when enough computing power is available to handle three space dimensions and a large ($\sim 10^6$) number of particles.

The analytical studies that gave so much insight into steady state systems (see eg. BT) are all too rare in the time dependent case. To our knowledge Kalnajs' (1973) model was the only one before this work wherein time dependent behaviour was studied analytically without approxiamtion. The work reported in this thesis has now added four distinct families of exact, analytic, time dependent models (described in detail in Chapter 3, Chapter 4 and Appendix A).

The shell models of Appendix A are cold, occupying a four dimensional surface in six dimensional phase space. Time dependent generalizations of Freeman's spheroid also occupy a four dimensional region, while the time dependent

generalizations of Polyachenko's "hot" spheroid occupy a five dimensional region. It is not clear whether these models will be stable to small disturbances. In any case, it seems hard to find situations in which such models could form and they should basically be regarded as illustrations of behaviour allowed by the CBE. Viewed as such, they demonstrate two interesting possibilities. (i) the existence of oscillating spheres with nonuniform density. This possibility was raised by Louis and Gerhard (1988) in their numerical work. (ii) The chaotic behaviour of the spheroid axes. This is very remniscent of anisotropic cosmological models which again reduce to Hamiltonian systems with a finite number of degrees of freedom (Misner 1969).

There are also two hot families, occupying a nonzero phase volume. The hot oscillating spheres have "inverted" phase space distribution functions and uniform real space density. In both these they differ from realistic galaxy models which have higher phase density at low energy and a strong decrease in real space density outside a central core. It is not clear whether the oscillations of uniform spheres found here will turn out to be stable and hence applicable to a wider class of models. This possibility is worth examining, perhaps in future numerical work. An undamped or weakly damped oscillation of a dark matter halo (for example) could be an energy input for gas flow in the time dependent potential.

The second hot system studied in this thesis is the

generalized Freeman disc. Again there are significant differences between these models and the phase space structure of more realistic bars. The stability is again an open question which will probably have to be answered by numerical studies. It is interesting that these model bars are stable under external harmonic potentials (these keep the model within the class of generalised Freeman discs). A more general stability analysis would be of great interest because bars are abundantly found in the real world.

Finally, the analytical study of a particular tidal encounter model in this thesis has allowed a convenient exploration of the validity of the impulse approximation, the effect of roation, and resonance effects between internal and orbital time scales. It will again be of interest to see how well this tractable model is able to mirror more realistic situations.

In brief, the new analytic models of time dependent stellar systems presented here have interesting properties in their own right and may also point to directions which need systematic explorations by numerical methods.